Quantum Dynamics in Nano-Scale Devices

Raedt, Hans De

Published in:
EPRINTS-BOOK-TITLE

Publication date:
1996

Published in: Computational Physics, 209 – 224,
ed. K.-H. Hoffmann and M. Schreiber, Springer 1996.

Quantum Dynamics in Nano-Scale Devices

HANS DE RAEDT

Institute for Theoretical Physics and Materials Science Centre
University of Groningen, Nijenborgh 4
NL-9747 AG Groningen, The Netherlands
E-mail: deraedt@phys.rug.nl

ABSTRACT

The purpose of this lecture is to introduce the general concepts for building algorithms to solve the time-dependent Schrödinger equation and to discuss ways of turning these concepts into unconditionally stable, accurate and efficient simulation algorithms. The approach is illustrated using results of a computer simulation study of charged-particle interferometry, combining features of both the Aharonov-Bohm and Hanbury Brown-Twiss experiment.

1. Introduction

Progress in nano-scale lithography has made it possible to perform "electron-optics" experiments in solid state devices[1,2]. In an ideal device the motion of the electrons is not affected by interactions with impurities, phonons etc., i.e. the electrons travel ballistically, just as they would do in ultra-high vacuum. In real devices, typical distances for ballistic motion can be as large as $250\lambda_F$, λ_F being the Fermi wavelength of the electrons[3].

A similar, but otherwise unrelated, break-through is the development of atom-size field-electron-emission sources. Recent experiments using these atom-size tips[4,5] have demonstrated that they act as unusual electron beam sources, emitting electrons at fairly low applied voltages (a few thousand volts or less) with a small angular spread (of a few degrees). These properties make such electron sources very attractive for applications to electron microscopy, holography and interferometry.

From physical point of view, both these nano-scale structures have at least one important common feature: The characteristic dimensions of these devices are comparable to the wavelength (typically the Fermi wavelength λ_F) of the relevant particles (typically electrons). Under this stringent condition, a classical, "billiard-ball" description of the particle motion is no longer valid. A calculation of the device properties requires a full quantum-mechanical treatment.

The dynamic properties of a non-relativistic quantum system is governed by the

time-dependent Schrödinger equation (TDSE)

$$i\hbar\frac{\partial}{\partial t}|\Phi(t)\rangle = \mathcal{H}|\Phi(t)\rangle \quad , \tag{1}$$

where $|\Phi(t)\rangle$ represents the state of the system described by the Hamiltonian $\mathcal{H}$ (here and in the following we use $\mathcal{H}$ to denote the differential operator and H for the hermitian matrix representing $\mathcal{H}$). In analogy with ordinary differential equations, the formal solution of the matrix differential equation

$$\frac{\partial}{\partial x}U(x) = HU(x) \quad ; \quad U(0) = I \quad , \tag{2}$$

where I denotes the $M \times M$ unit matrix and H is a $M \times M$ matrix, is given by

$$U(x) = e^{xH} \quad , \tag{3}$$

and is called the exponential of the matrix H. In quantum physics and quantum statistical mechanics, the exponential of the Hamiltonian is a fundamental quantity. All methods for solving these problems compute, one way or another, (matrix elements of) the exponential of the matrix H. In the case of real-time quantum dynamics $x = -it/\hbar$ whereas for quantum statistical problems $x = -\beta = -1/k_BT$.

Formally, the exponential of a matrix H can be defined in terms of the Taylor series

$$e^{xH} = \sum_{n=0}^{\infty}\frac{x^n}{n!}H^n \quad , \tag{4}$$

just like if H would be a number. For most problems of interest, there won't be enough memory to store the matrix H (typical applications require matrices of dimension $10^5 \times 10^5$ or larger) and hence there also will be no memory to store the full matrix e^{xH}. So let us concentrate on the other extreme: The calculation of an arbitrary matrix element $\langle\psi|e^{xH}|\psi'\rangle$. Although from mathematical point of view, formal expansion (4) is all that is really needed, when it comes to computation, (4) is quite useless. The reason is not so much that it is a Taylor series but rather that it contains powers of the matrix, indicating that simply summing the terms in (4) may be very inefficient (and indeed it is).

There is one particular case in which it is easy to compute the matrix element $\langle\psi|e^{xH}|\psi'\rangle$ namely if *all* the eigenvalues and eigenvectors are known. Indeed, from (4) it follows that

$$e^{xH}|\Phi_j\rangle = \sum_{n=0}^{\infty}\frac{x^n}{n!}H^n|\Phi_j\rangle = \sum_{n=0}^{\infty}\frac{x^n}{n!}E_j^n|\Phi_j\rangle = e^{xE_j}|\Phi_j\rangle \quad , \tag{5}$$

where (here and in the following) E_n denotes the n-th eigenvalue of the matrix H

and $|\Phi_n\rangle$ is the corresponding eigenvector. We will label the eigenvalues such that $E_0 \leq E_1 \leq \ldots \leq E_{M-1}$ where M is the dimension of the matrix H. From (5) is follows that

$$\langle\psi|e^{xH}|\psi'\rangle = \sum_{j=0}^{M-1} \langle\psi|\Phi_j\rangle\langle\Phi_j|\psi'\rangle e^{xE_j} \quad . \tag{6}$$

Of course, result (6) is almost trivial but it is important to keep in mind that, except for some pathological cases, there seems to be no other practical way to compute the matrix element $\langle\psi|e^{xH}|\psi'\rangle$ without making approximations (assuming H is a large matrix). In general we don't know the solution of the eigenvalue problem of the matrix H, otherwise we would already have solved the most difficult part of the whole problem. Therefore (6) is not of practical use.

Solving the time-dependent Schrödinger equation for even a single particle moving in a non-trivial (electromagnetic) potential is not a simple matter. The main reason is that for most problems of interest, the dimension of the matrix representing $\mathcal{H}$ is quite large and although the dimension of the matrices involved is certainly not as large as in the case of typical many-body quantum systems, exact diagonalization techniques are quite useless. Indeed, a calculation of the time-development of the wave function by exact diagonalization techniques requires the knowledge of *all* eigenvectors and *all* eigenvalues (i.e. $\approx 10^{13}$ Mb or more RAM to store these data). Thus, we need algorithms that do not use more than $\mathcal{O}(M+1)$ storage elements. Diagonalization methods that only require $\mathcal{O}(M+1)$ memory locations are of no use either because they can only compute a (small) part of the spectrum. Methods based on importance sampling concepts cannot be employed at all because there is no criterion to decide which state is important or which is not: The "weight" of a state $e^{-itE_j/\hbar}$ is a complex number of "size" one.

Although from numerical point of view the TDSE looks like any other differential equation which one should be able to solve by standard methods (Runge-Kutta, ...) this similarity is misleading. Standard methods are based on (clever) truncations of the Taylor series expansion. It is easy to convince oneself that, for the TDSE, this implies that these numerical algorithms do not conserve the norm of the wave function.[6] This, from physical point of view, is unacceptable because it means that during the numerical solution of the TDSE, the number of particles will change. Moreover, it can be shown[6] that this implies that these methods are not always stable with respect to rounding and other numerical errors. For completeness it should be mentioned that the Cranck-Nicholson algorithm does conserve the norm of the wave function and is unconditionally stable. However, except for one-dimensional problems, in terms of accuracy and efficiency it cannot compete with the algorithms to be discussed below.[6]

A key concept in the construction of an algorithm for solving the TDSE is the so-

called unconditional stability. An algorithm for solving the TDSE is unconditionally stable if the norm of the wavefunction is conserved *exactly*, at *all* times.[6] From physical point of view, unconditional stability obviously is an essential requirement. If an algorithm is unconditionally stable the errors due to rounding, discretization etc. never run out of hand, irrespective of the choice of the grid, the time step, or the number of propagation steps. Recall that the formal solution of the TDSE is given by

$$|\Phi(m\tau)\rangle = e^{-im\tau H}|\Phi(t=0)\rangle \quad , \tag{7}$$

where $m = 0, 1, \ldots$ counts the number of time-steps τ. Here and in the following we absorb $\hbar$ in τ.

A simple, general recipe for constructing an unconditionally stable algorithm is to use unitary approximations to the (unitary) time-step operator $U(\tau) = e^{-i\tau H}$.[6] The Trotter-Suzuki product formula approach, to be discussed in the next section, provides the necessary mathematical framework for constructing unconditionally stable, accurate and efficient algorithms to solve the TDSE.[6]

2. Theory

In all cases that we know of, the Hamiltonian is a sum of several contributions and each contribution itself is usually simple enough so that we can diagonalize it ourselves by some (simple) transformation. The Hamiltonian for a particle in a potential provides the most obvious example: We can write the Hamiltonian as a sum of the free-particle Hamiltonian and a potential energy. It is trivial to diagonalize both parts independently but it is usually impossible to diagonalize the sum.

The question we can now put ourselves is the following. Suppose we can diagonalize each of the terms in H by hand. Then, it is very reasonable to assume that we can also compute the exponential of each of the contributions separately (see the discussion in the previous section). Is there then a relation between the exponentials of each of the contributions to H and the exponential of H and if so, can we use it to compute the latter ?

The answer to this question is affirmative and can be found in the mathematical literature of the previous century. The following fundamental result due to Lie,[7] is the basis for the Trotter-Suzuki method for solving quantum problems.[8,9,10] It expresses the exponential of a sum of two matrices as infinite ordered product of the exponentials of the two individual matrices:

$$e^{x(A+B)} = \lim_{m\to\infty} \left(e^{xA/m} e^{xB/m}\right)^m \quad , \tag{8}$$

where, for our purposes, A and B are $M \times M$ matrices. The result (8) is called the

Trotter formula. A first hint for understanding why (8) holds comes from comparing the two Taylor series

$$\begin{aligned} e^{x(A+B)/m} &= I + \frac{x}{m}(A+B) + \frac{1}{2}\frac{x^2}{m^2}(A+B)^2 + \mathcal{O}(x^3/m^3) \\ &= I + \frac{x}{m}(A+B) \\ &\quad + \frac{1}{2}\frac{x^2}{m^2}(A^2 + AB + BA + B^2) + \mathcal{O}(x^3/m^3) \quad , \end{aligned} \tag{9a}$$

and

$$e^{xA/m}e^{xB/m} = I + \frac{x}{m}(A+B) + \frac{1}{2}\frac{x^2}{m^2}(A^2 + 2AB + B^2) + \mathcal{O}(x^3/m^3) \quad . \tag{9b}$$

It is clear that for sufficiently large m, both expansions will agree up to terms of $\mathcal{O}(x^2\|[A,B]\|/m^2)$.[11] Thus, for sufficiently large m (how large depends on x and $\|[A,B]\|$),

$$e^{x(A+B)/m} \approx e^{xA/m}e^{xB/m} \quad . \tag{10}$$

A mathematically rigorous treatment shows that[12]

$$\|e^{x(A+B)/m} - e^{xA/m}e^{xB/m}\| \leq \frac{x^2}{2m^2}\|[A,B]\|e^{|x|(\|A\|+\|B\|)/m} \quad , \tag{11}$$

demonstrating that for finite m, the difference between the exponential of a sum of two matrices and the ordered product of the individual exponentials vanishes as x^2/m. As expected, (11) also reveals that this difference is zero if A and B commute: If $[A,B]=0$ then $e^{x(A+B)} = e^{xA}e^{xB}$. For the case at hand $x = -im\tau$ and then upperbound in (11) can be improved considerably to read[6]

$$\|e^{-i\tau(A+B)} - e^{-i\tau A}e^{-i\tau B}\| \leq \frac{\tau^2}{2}\|[A,B]\| \quad , \tag{12}$$

Except for the fact that we assumed that $H = A+B$, the above discussion has been extremely general. This suggests that one can apply the Trotter-Suzuki approach to a wide variety of problems and indeed one can. We have only discussed the most simple form of the Trotter formula. There now exist a vast number of extensions and generalizations of which we will consider only three of them.

The Trotter formula is readily generalized to the case of more than two contributions to H. Writing $H = \sum_{i=1}^{p} A_i$ it can be shown that[6,12]

$$\|e^{-i\tau(A_1+\ldots+A_p)} - e^{-i\tau A_1}\ldots e^{-i\tau A_p}\| \leq \frac{\tau^2}{2}\sum_{1\leq i<j\leq p}\|[A_i,A_j]\| \quad , \tag{13}$$

showing that *any* decomposition of the Hamiltonian qualifies as a candidate for applying the Trotter-Suzuki approach. This is an important conclusion because the flexibility of choosing the decomposition of H can be exploited to construct efficient algorithms. From the above discussion it is also clear that at no point, an assumption was made about the "importance" of a particular contribution to H. This is the reason why the Trotter-Suzuki approach can be used where perturbation methods break down.

The product formula (10) is the simplest one can think of. We use it to define an approximate time-step operator

$$U_1(\tau) = e^{-i\tau A_1} \dots e^{-i\tau A_p} \quad . \tag{14}$$

The hermitian conjugate of this operator is given by

$$U_1^\dagger(\tau) = e^{i\tau A_p} \dots e^{i\tau A_1} \quad , \tag{15}$$

from which it follows that

$$U_1(\tau) U_1^\dagger(\tau) = I \quad . \tag{16}$$

For simplicity we have assumed that H has be written as a sum of hermitian contributions, i.e. $A_i = A_i^\dagger$ for $i = 1, \dots, p$. Result (16) implies that $(U_1(\tau))^{-1} = U_1^\dagger(\tau)$ hence $U_1(\tau)$ is a unitary approximation to the time-step operator $e^{-i\tau H}$. Thus, if we succeed in implementing $U_1(\tau)$, the resulting algorithm will be unconditionally stable by construction. The upperbound in (13) shows that the error made by replacing $e^{-i\tau H}$ by $U_1(\tau)$ will, in the worst case, never exceed a constant multiplied by τ^2. Therefore $U_1(\tau)$ is said to be a first-order approximant to the time-step operator.

For many applications it is necessary to employ an algorithm that is correct up to fourth order in the time step. Approximants correct up to second order are obtained by symmetrization[6,12,13]

$$U_2\ (\tau) = U_1^T(\tau/2) U_1\ (\tau/2) \quad , \tag{17}$$

where the U_1^T is the transpose of U_1 . Trotter-Suzuki formula-based procedures to construct algorithms that are correct up to fourth-order in the time step are given in ref.6. From practical point of view, a disadvantage of the fourth-order methods introduced in ref.6 is that they involve commutators of various contributions to the Hamiltonian. Recently Suzuki proposed a symmetrized fractal decomposition of the time evolution operator.[14] Using this formula, a fourth-order algorithm is easily build from a second-order algorithm by applying[14]

$$U_4(\tau) = U_2(p\tau) U_2(p\tau) U_2((1-4p)\tau) U_2(p\tau) U_2(p\tau) \quad , \tag{18}$$

where $p = 1/(4 - 4^{1/3})$ and $U_n(\tau)$ is the n–th order approximation to $U(\tau)$, i.e. $U(\tau) = U_n(\tau) + \mathcal{O}(\tau^{n+1})$. It is trivial to show that all of the above approximations are unitary operators, hence the corresponding algorithms will be unconditionally stable. Note that once we have programmed a first-order algorithm, writing the code to implement the second- and fourth-order algorithms will normally only take a few seconds.

3. Data analysis

The amount of data generated by a TDSE solver can be tremendous: The wave function is known at each time step so that in principle the TDSE solver can generate $\mathcal{O}(16mM)$ bytes of data in a single run. In typical applications, $M \approx 10^6$ and $m > 1000$. Clearly it may be difficult to store all these data. Therefore it is more appropriate to process the data as it is generated and compress it as much as possible.

A very appealing method to look at the data is to make say 100 snapshots of the (coarse grained) probability distribution and to use visualization techniques to produce digital video's.[15,16,17] Simply looking at these video's can already bring a lot of insight but, to be on the save side, this insight should be confronted with the results of more advanced, numerical processing of the data.

The numerical processing of the raw data generated by the TDSE solver depends to considerable extent on the details of the actual application. Therefore I will not dwell on this subject in full generality but confine myself to a discussion of a simple, widely applicable method to extract from the raw data, information about the spectrum of the model Hamiltonian.

The idea is straightforward. Consider the matrix element $\langle\Phi(t=0)|\Phi(t)\rangle$ and write $|\Phi(t)\rangle$ in terms of the (unknown) eigenvalues and eigenvectors of H to obtain

$$f(t) \equiv \langle\Phi(t=0)|\Phi(t)\rangle = \sum_{j=0}^{M-1} |\langle\Phi(t=0)|\Phi_j\rangle|^2 e^{-itE_j} \quad . \tag{19}$$

From (19) it is clear that the Fourier transform of $f(t)$ with respect to t will give direct information on all the E_j's for which the overlap $|\langle\Phi(t=0)|\Phi_j\rangle|^2$ is not negligible. In other words, if we keep all the values of $f(t = m\tau)$ and compute the its Fourier transform, we obtain the local (with respect to the initial state $\Phi(t=0)$) density of states.

4. Implementation

In general there will be many possibilities to write down different decompositions of a given Hamiltonian. From theoretical point of view, the choice of the

decomposition is arbitrary. In practice however, this flexibility can be exploited to considerable extent to tailor the algorithm to the computer architecture on which the algorithm will execute. Of particular interest are decompositions that vectorize well and have a large intrinsic degree of parallelism.

We now illustrate the application of the theory presented above to the case of a charged (spinless) non-relativistic particle in an external, static magnetic field $\mathbf{B}$. The hamiltonian reads

$$\mathcal{H} = \frac{1}{2m^*} \left(\mathbf{p} \ - e\mathbf{A} \ \right)^2 + V \quad , \tag{20}$$

where m^* is the effective mass of the particle with charge e, $\mathbf{p} \ = -i\hbar\nabla$ is the momentum operator, $\mathbf{A}$ represents the vector potential and V denotes the potential. For many applications it is sufficient to consider the choice $\mathbf{B} \ = (0, 0, B(x, y))$ and $V = V(x, y)$. Then the problem is essentially two-dimensional and the motion of the particle may be confined to the x–y plane. For numerical work, there is no compelling reason to adopt the Coulomb gauge (div$\mathbf{A} \ = 0$). A convenient choice for the vector potential is $\mathbf{A} \ = (A_x(x, y), 0, 0)$ where

$$A_x(x, y) = -\int_0^y B(x, y)\, dy \quad . \tag{21}$$

We will solve the TDSE for the Hamiltonian (20) with the boundary condition that the wave function is zero outside the simulation box, i.e. we assume perfectly reflecting boundaries.

For computational purposes it is expedient to express all quantities in dimensionless units. Fixing the unit of length by λ, wavevectors are measured in units of $k = 2\pi/\lambda$, energies in $E = \hbar^2k^2/2m^*$, time in $\hbar/E$ and the vector potential in $e\lambda/\hbar$. Expressed in these dimensionless variables Hamiltonian (20) reads

$$\mathcal{H} = -\frac{1}{4\pi^2} \left\{ \left[\frac{\partial}{\partial x} - iA_x(x, y) \right]^2 + \frac{\partial^2}{\partial y^2} \right\} + V(x, y) \quad . \tag{22}$$

An essential step in the construction of a numerical algorithm is to discretize the derivatives with respect to the x and y coordinates (of course, if the problem is defined on a lattice instead of in continuum space this step can be omitted). For many purposes, it is necessary to use a difference formula for the first and second derivatives in (22) that is accurate up to fourth order in the spatial mesh size δ. Using the standard four and five point difference formula[18] the discretized r.h.s. of (22) reads

$$H\Phi_{l,k}(t) = \frac{1}{48\pi^2\delta^2} \Big\{ \quad \Big[1 - i\delta\big(A_{l,k} + A_{l+2,k}\big)\Big] \Phi_{l+2,k}(t)$$

$$
\begin{aligned}
&+\Big[1+i\delta\big(A_{l-2,k}+A_{l,k}\big)\Big]\Phi_{l-2,k}(t)\\
&-16\Big[1-\frac{i\delta}{2}\big(A_{l,k}+A_{l+1,k}\big)\Big]\Phi_{l+1,k}(t)\\
&-16\Big[1+\frac{i\delta}{2}\big(A_{l-1,k}+A_{l,k}\big)\Big]\Phi_{l-1,k}(t)\\
&+\Phi_{l,k+2}+\Phi_{l,k-2}-16\Phi_{l,k+1}-16\Phi_{l,k-1}(t)\\
&+\Big[60+12\delta^2A_{l,k}^2+48\pi^2\delta^2V_{l,k}\Big]\Phi_{l,k}(t)\Big\}+\mathcal{O}(\delta^5) \quad , \quad (23)
\end{aligned}
$$

where $\Phi_{l,k}(t) = \Phi(l\delta, k\delta, t)$ and $A_{l,k} = A_x(l\delta, k\delta)$. The discretized form (23) will provide a good approximation to the continuum problem if δ is substantially smaller than the smallest physical length scale. For the case at hand there are two such scales. One is the de Broglie wavelength of the particle (which by definition is equal to λ) and the other is the (smallest) magnetic length defined by $l_B^2 = \min_{(x,y)} |\hbar/eB(x,y)|$. From numerical calculations (not shown) it follows that $\delta = 0.1\min(1, l_B)$ yields a good compromise between accuracy and the CPU time required to solve the TDSE.

Straightforward application of the product-formula recipe to expression (23) requires a cumbersome matrix notation. This can be avoided in the following way.[6] Defining

$$
|\Phi(t)\rangle = \sum_{l=1}^{L_x}\sum_{k=1}^{L_y}\Phi_{l,k}(t)c_{l,k}^{+}|0\rangle \quad , \quad (24)
$$

where L_x and L_y are the number of grid points in the x and y direction respectively and $c_{l,k}^{+}$ creates a particle at lattice site (l,k), (24) can be written as

$$
|\Phi(m\tau)\rangle = e^{-im\tau H}|\Phi(t=0)\rangle \quad , \quad (25)
$$

where

$$
\begin{aligned}
H = \frac{1}{48\pi^2\delta^2}\sum_{l=1}^{L_x-2}\sum_{k=1}^{L_y}\Big\{&\Big[1-i\delta\big(A_{l,k}+A_{l+2,k}\big)\Big]c_{l,k}^{+}c_{l+2,k}\\
&+\Big[1+i\delta\big(A_{l,k}+A_{l+2,k}\big)\Big]c_{l+2,k}^{+}c_{l,k}\Big\}\\
-\frac{1}{3\pi^2\delta^2}\sum_{l=1}^{L_x-1}\sum_{k=1}^{L_y}\Big\{&\Big[1-\frac{i\delta}{2}\big(A_{l,k}+A_{l+1,k}\big)\Big]c_{l,k}^{+}c_{l+1,k}\\
&+\Big[1+\frac{i\delta}{2}\big(A_{l,k}+A_{l+1,k}\big)\Big]c_{l+1,k}^{+}c_{l,k}\Big\}
\end{aligned}
$$

$$+\frac{1}{48\pi^2\delta^2}\sum_{l=1}^{L_x}\sum_{k=1}^{L_y-2}\left(c^+_{l,k}c_{l,k+2}+c^+_{l,k+2}c_{l,k}\right)$$
$$-\frac{1}{3\pi^2\delta^2}\sum_{l=1}^{L_x}\sum_{k=1}^{L_y-1}\left(c^+_{l,k}c_{l,k+1}+c^+_{l,k+1}c_{l,k}\right)$$
$$+\frac{1}{48\pi^2\delta^2}\sum_{l=1}^{L_x}\sum_{k=1}^{L_y}\left(60+12\delta^2A^2_{l,k}+48\pi^2\delta^2V_{l,k}\right)+\mathcal{O}(\delta^5) \quad , \qquad (26)$$

where $c_{l,k}$ annihilates a particle at lattice site (l,k).

Hamiltonian (26) describes a particle that moves on a two-dimensional lattice by making nearest and next-nearest neighbor jumps. This interpretation suggests that H should be written as a sum of terms that represent groups of independent jumps.[6] A convenient choice is

$$A_1=\frac{1}{48\pi^2\delta^2}\sum_{l\in X_1}\sum_{k=1}^{L_y}\Big\{\Big[1-i\delta\big(A_{l,k}+A_{l+2,k}\big)\Big]c^+_{l,k}c_{l+2,k}$$
$$+\Big[1+i\delta\big(A_{l,k}+A_{l+2,k}\big)\Big]c^+_{l+2,k}c_{l,k}\Big\} \quad ;$$
$$X_1=\{1,2,5,6,9,10,\ldots\} \quad ,$$
$$A_2=\frac{1}{48\pi^2\delta^2}\sum_{k=1}^{L_y}\sum_{l\in X_2}\Big\{\Big[1-i\delta\big(A_{l,k}+A_{l+2,k}\big)\Big]c^+_{l,k}c_{l+2,k}$$
$$+\Big[1+i\delta\big(A_{l,k}+A_{l+2,k}\big)\Big]c^+_{l+2,k}c_{l,k}\Big\} \quad ;$$
$$X_2=\{3,4,7,8,11,12,\ldots\} \quad ,$$
$$A_3=\frac{-1}{3\pi^2\delta^2}\sum_{k=1}^{L_y}\sum_{l\in X_3}\Big\{\Big[1-\frac{i\delta}{2}\big(A_{l,k}+A_{l+1,k}\big)\Big]c^+_{l,k}c_{l+1,k}$$
$$+\Big[1+\frac{i\delta}{2}\big(A_{l,k}+A_{l+1,k}\big)\Big]c^+_{l+1,k}c_{l,k}\Big\} \quad ;$$
$$X_3=\{1,3,5,7,9,11,\ldots\} \quad ,$$
$$A_4=\frac{-1}{3\pi^2\delta^2}\sum_{k=1}^{L_y}\sum_{l\in X_4}\Big\{\Big[1-\frac{i\delta}{2}\big(A_{l,k}+A_{l+1,k}\big)\Big]c^+_{l,k}c_{l+1,k}$$
$$+\Big[1+\frac{i\delta}{2}\big(A_{l,k}+A_{l+1,k}\big)\Big]c^+_{l+1,k}c_{l,k}\Big\} \quad ;$$
$$X_4=\{2,4,6,8,10,12,\ldots\} \quad ,$$

$$A_5 = \frac{1}{48\pi^2\delta^2} \sum_{k\in X_5} \sum_{l=1}^{L_x} \big(c^+_{l,k}c_{l,k+2} + c^+_{l,k+2}c_{l,k}\big) \quad ; \quad X_5 = \{1,2,5,6,9,10,\ldots\} \quad ,$$

$$A_6 = \frac{1}{48\pi^2\delta^2} \sum_{k\in X_6} \sum_{l=1}^{L_x} \big(c^+_{l,k}c_{l,k+2} + c^+_{l,k+2}c_{l,k}\big) \quad ; \quad X_6 = \{3,4,7,8,11,12,\ldots\} \quad ,$$

$$A_7 = \frac{-1}{3\pi^2\delta^2} \sum_{k\in X_3} \sum_{l=1}^{L_x} \big(c^+_{l,k}c_{l,k+1} + c^+_{l,k+1}c_{l,k}\big) \quad ; \quad X_3 = \{1,3,5,7,9,11,\ldots\} \quad ,$$

$$A_8 = \frac{-1}{3\pi^2\delta^2} \sum_{k\in X_4} \sum_{l=1}^{L_x} \big(c^+_{l,k}c_{l,k+1} + c^+_{l,k+1}c_{l,k}\big) \quad ; \quad X_4 = \{2,4,6,8,10,12,\ldots\} \quad ,$$

$$A_9 = \frac{1}{48\pi^2\delta^2} \sum_{k=1}^{L_y} \sum_{l=1}^{L_x} \big(60 + 12\delta^2 A^2_{l,k} + 48\pi^2\delta^2 V_{l,k}\big) \quad , \tag{27}$$

and

$$U_1(\tau) = \prod_{n=1}^{9} e^{-i\tau A_n} \quad , \tag{28}$$

is the first-order approximant from which the algorithm, correct up to fourth-order in the spatial (δ) and temporal (τ) mesh size, can be build.

Inspection of A_n for $n = 1,\ldots,9$ shows that each of the terms commutes with all the other terms in the sum over k and l. This is because each of these terms corresponds to a jump of the particle between a pair of two, isolated sites. For the purpose of implementation, this feature is of extreme importance.[6] To illustrate this point it is sufficient to consider the first of the exponents in (28) and use the fact that all terms commute to rewrite it as

$$e^{-i\tau A_1} = \prod_{k=1}^{L_y} \prod_{l\in X_1} \exp\Bigg(\frac{-i\tau}{48\pi^2\delta^2} \Big\{ \Big[1 - i\delta\big(A_{l,k} + A_{l+2,k}\big)\Big] c^+_{l,k}c_{l+2,k} + \Big[1 + i\delta\big(A_{l,k} + A_{l+2,k}\big)\Big] c^+_{l+2,k}c_{l,k} \Big\} \Bigg) \quad . \tag{29}$$

Furthermore, each of the exponents in the product (29) describes a two-site system, and the exponent of the corresponding two-by-two matrix can be worked out analytically.[6] In general

$$\begin{aligned} \exp\big(i\tau\alpha c^+_{l,k}c_{l',k'} + i\tau\alpha^* c^+_{l',k'}c_{l,k}\big) =& \big(c^+_{l,k}c_{l,k} + c^+_{l',k'}c_{l',k'}\big)\cos\tau|\alpha| \\ &+ i\big(\alpha^{*-1}c^+_{l,k}c_{l',k'} + \alpha^{-1}c^+_{l',k'}c_{l,k}\big)\sin\tau|\alpha| \end{aligned} \tag{30}$$

The rather formal language used above easily translates into a computer pro-

gram. All that (27)–(30) imply is that for each factor in product formula (28) one has to pick successive pairs of lattice points, get the values of the wave function for each pair of points and perform a plane rotation using matrices of the form

$$M = \begin{pmatrix} \cos\tau|\alpha| & +i\alpha^{-1}\sin\tau|\alpha| \\ +i\alpha^{*-1}\sin\tau|\alpha| & \cos\tau|\alpha| \end{pmatrix} \quad . \tag{31}$$

For each of the nine exponentials,[19] the order in which the pairs of points are processed is irrelevant. Therefore, the computation of each of the nine factors can be done entirely parallel, fully vectorized, or mixed parallel and vectorized depending on the computer architecture on which the code will execute. Further technical details on the implementation of this algorithm can be found elsewhere.[20]

5. Quantum interference of two identical particles

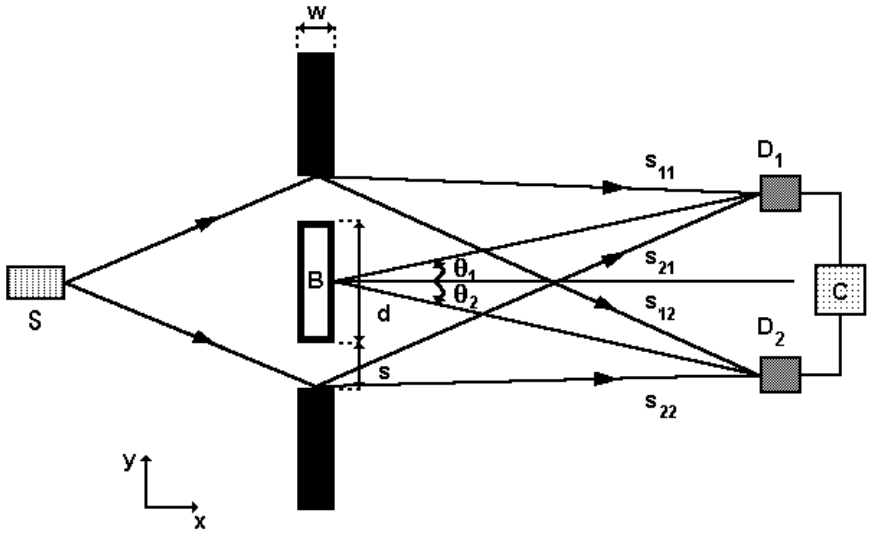

Fig.1. Schematic view of the combined Aharonov-Bohm – Hanbury-Brown Twiss apparatus. Charged fermions or bosons leave the source S, pass through the double-slit and arrive at detectors D_1 and D_2. The signals of these detectors are multiplied in correlator C. The particles do not experience the magnetic field B enclosed in the double-slit apparatus.

Trotter-Suzuki based TDSE solvers have been employed to study a variety of problems including wave localization in disordered and fractals,[6,21] electron emission from nanotips,[22,23,15] Andreev reflection in mesoscopic systems,[24,16] the Aharonov-Bohm effect,[20,17] quantum interference of charged identical particles,[25,17] etc.. Appealing features of the TDSE approach are that is extremely flexible in the

sense that it can handle arbitrary geometries and (vector) potentials and that its numerical stability and accuracy are such that for all practical purposes the solution is exact.

Trotter-Suzuki formula-based algorithms can and also have been used to solve the TDSE for few-body quantum systems, including a 26-site S=1/2 Heisenberg model.[26] The application of the TDSE approach is mainly limited by the storage needed for the (complex valued) wave function.

In this section we will use the TDSE approach to study some aspects of quantum interference of charged identical particles. Recently Silverman[27,28] proposed and analyzed a thought experiment that combines both the features of the Aharonov-Bohm (AB) and Hanbury-Brown and Twiss (HBT) experiments. The former provides information on the effect of the magnetic field on correlations of two *amplitudes*. The latter on the other hand yields direct information on the correlations of two *intensities*, i.e. of correlations of *four* amplitudes.

A schematic view of the AB-HBT apparatus is shown in Fig.1. Charged fermions or bosons leave the source S, pass through the double-slit and arrive at detectors D_1 and D_2. In order for the particle statistics to be relevant at all, it is necessary that in the detection area the wave functions of two individual particles overlap. For simplicity, it is assumed that the particles do not interact. The particle statistics may affect the single-particle as well as two-particle interference. The former can be studied by considering the signal of only one of the two detectors. Information on the latter is contained in the cross-correlation of the signals of both detectors. Below we report some of our results[25] for the AB-HBT thought experiment, as obtained from the numerically exact solution of the time-dependent Schrödinger equation (TDSE) using the algorithm described above.

In practice we solve the two-particle TDSE subject to the boundary condition that the wave function is zero outside the simulation box (a grid of 1024×513 points), i.e. we assume perfectly reflecting boundaries. The algorithm that we use is accurate to fourth-order in both the spatial and temporal mesh size.[20] Additional technical details can be found elsewehere.[20] Physical properties are calculated from the two-particle amplitude $\Phi(\mathbf{r},\mathbf{r}',t) = \phi_1(\mathbf{r},t)\phi_2(\mathbf{r}',t) \pm \phi_2(\mathbf{r},t)\phi_1(\mathbf{r}',t)$ where $\phi_1(\mathbf{r},t)$ and $\phi_2(\mathbf{r},t)$ are the single-particle amplitudes and the plus and minus sign correspond to the case of bosons and fermions respectively.

Let us first reproduce Silverman's analysis.[27,28] Assume that the double-slit apparatus can be designed such that the probability for two identical particles (fermions or bosons) to pass through the same slit can be made negligibly small. The two slits then act as the two sources in the HBT experiment with one modification: Due to the presence of the vector potential the waves can pick up an extra phase shift. According to Silverman,[27,28] it immediately follows that the signal generated by the cross-correlator will *not* show any dependence on the confined magnetic field. The AB shifts for the direct process and the one in which the identical particles

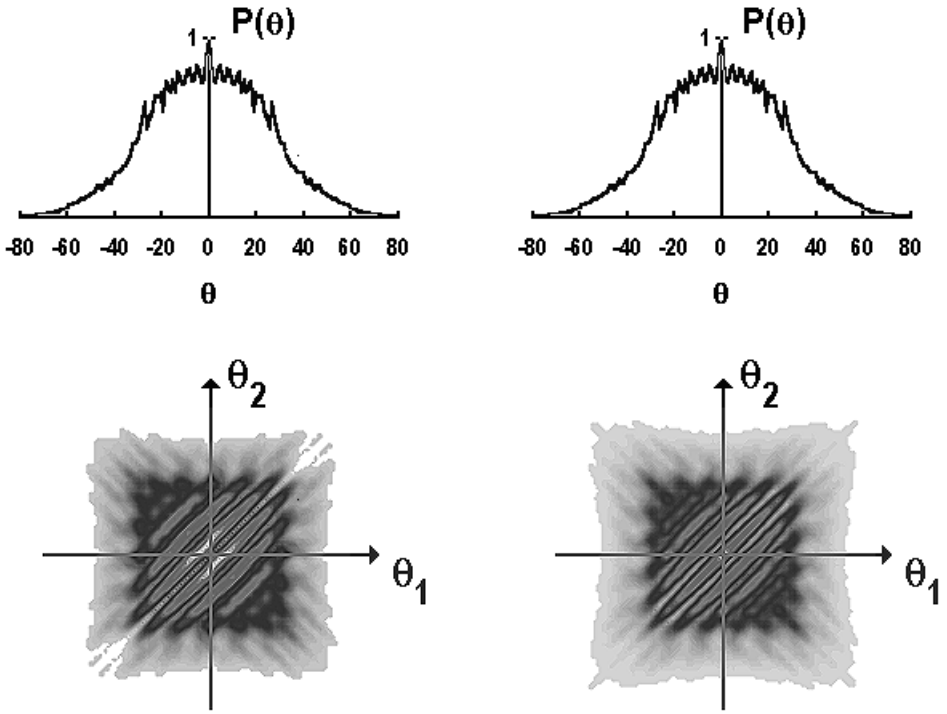

Fig.2. Simulation results for single- (top) and correlated (bottom) detector signal for $B = 0$, obtained from the solution of the TDSE for the initial state as described in the text. Left: Signals generated by fermions. Right: Signals generated by bosons. The corresponding pictures for $B = B_0{}^{(30)}$ are identical and not shown.

have been interchanged mutually cancel. This cancelation is independent of the fact that the particles are fermions or bosons.[29]

The basic assumption of Silverman's analysis is easily incorporated into a computer experiment. The initial two-particle wave function is a properly symmetrized product of single-particle wave functions which, for simplicity, are taken to be Gaussians. Each Gaussian is positioned such that during propagation it effectively "hits" only one slit. The single (top) and correlated (bottom) signals, received by detectors placed far to the right of the slits for $B = 0$ for fermions (l.h.s) as well as for bosons (r.h.s.) are shown in Fig.2.

For fermions the correlated signal for $\theta_1 = \theta_2$ vanishes, as required by the Pauli principle. This feature is hardly visible, due to the resolution we used to generate the pictures but it is present in the raw data. Within four digit accuracy, the corresponding data for $B = B_0$ (or, as a matter of fact, for any B) are identical to those for $B = 0$.[25] Comparison of the cross-correlated intensities (bottom part) clearly lends support to Silverman's conclusion.[27,28] However, it is also clear that the single-detector signals (upper part) do *not* exhibit the features characteristic of

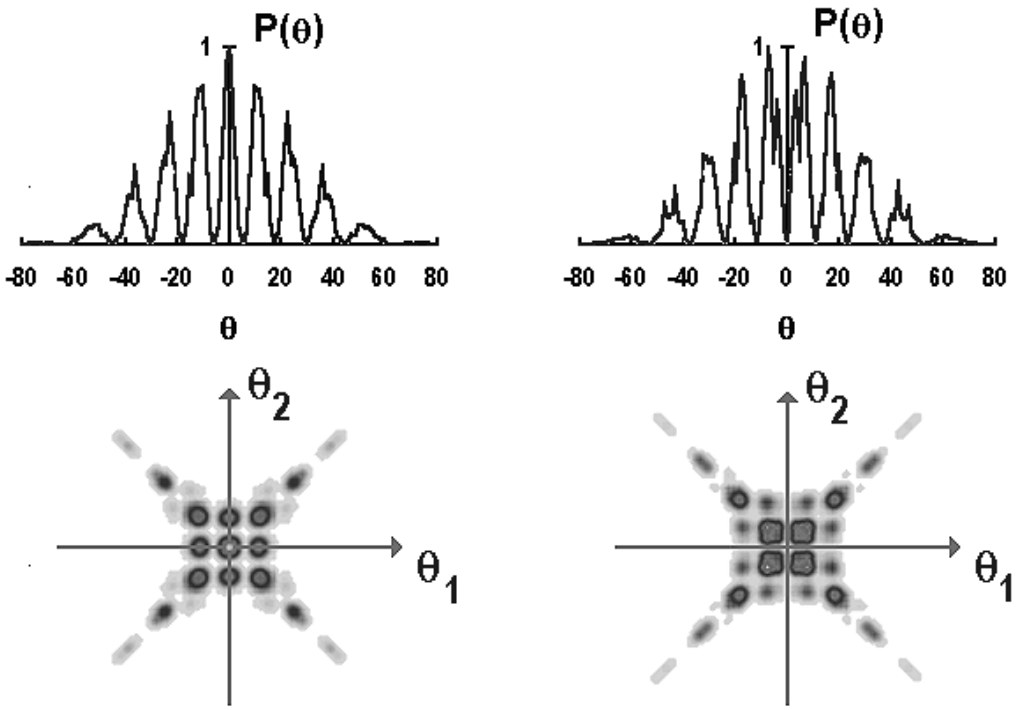

Fig.3. Simulation results for single- (top) and correlated (bottom) detector signal generated by two bosons, as obtained from the solution of the TDSE for the initial state described in the text. Left: $B = 0$. Right: $B = B_0$.

the AB effect. Under the conditions envisaged by Silverman, not only is there no AB effect in the cross-correlated signal: There is no AB effect at all.

The absence of the AB effect can be traced back to Silvermans's assumption that the slits can be regarded as sources, thereby eliminating the second, topologically different, alternative for a particle to reach the detector. A different route to arrive at the same conclusion is to invoke gauge invariance to choose the vector potential such that the two particles would never experience a non-zero vector potential.

A full treatment of the thought experiment depicted in Fig.1 requires that *all* possibilities for *both* identical particles are included in the analysis. This is easily done in the computer experiment by changing the position and width of the Gaussians used to build the initial wave function of the fermions or bosons such that they both hit the two slits. Some of our results for the case of two bosons are shown in Fig.3. Comparison of the upper parts of Fig.3 provides direct evidence of the presence of the AB effect.

The cross-correlated boson intensities (r.h.s. of the bottom part of Fig.3) clearly exhibit an AB-like effect. The positions of the maxima and minima are interchanged if the magnetic field changes from $B = 0$ to $B = B_0$. We have verified that the

shift of these positions is a periodic function of the field B. These results for the case of boson statistics cannot be explained on the basis of Silverman's theory.[27,28]

In general we find that there is only a small quantitative difference between the fermion and boson single-detector signals: The interference fringes of the fermions are less pronounced than in the case of bosons, another manifestation of the Pauli principle. The differences in the cross-correlated fermion intensities, due to B, are not as clear as in the boson case. Substracting the $B = 0$ from the $B = B_0$ signal and plotting the absolute value of this difference (not shown) clearly shows that also the cross-correlated fermion intensity exhibits features that are characteristic of the AB effect.[25] The high symmetry in all the correlated signals shown is due to our choice $B = 0, B_0$. The fact that we recover this symmetry in our simulation data provides an extra check on our method. If B is not a multiple of B_0, this high symmetry is lost but the salient features of the signals remain the same. From our numerical experiments, we conclude that in an AB-HBT experiment, an AB shift of the interference pattern will be observed in both the single and two-detector experiments. The AB effect (in both experiments) is more pronounced for bosons than for fermions.

6. Acknowledgements

Most of the material used for this paper is taken from work done in collaboration with K. Michielsen. I would like to thank K. Michielsen for a critical reading of the manuscript. Financial support by the "Stichting voor Fundamenteel Onderzoek der Materie (FOM)", which is financially supported by the "Nederlandse Organisatie voor We-tenschappelijk Onderzoek (NWO)", the "Stichting Nationale Computer Faciliteiten (NCF)", and the EEC is gratefully acknowledged.

7. References

1. S. Washburn, *Nature* **343** (1990) 415.
2. H. van Houten, C.W.J. Beenakker, and B.J. van Wees, *Semiconductors and Semimetals*, edited by M.A. Reed, (New York, Academic 1990).
3. H. van Houten et al., *Phys. Rev. B* **39** (1989) 8556.
4. Vu Thien Binh and J. Marien, *Surface Science* **102** (1988) L539.
5. Vu Thien Binh, *J. Microscopy* **152** (1988) 355.
6. H. De Raedt, *Comp. Phys. Rep.* **7** (1987) 1.
7. S. Lie and F. Engel, *Theorie der Transformationgruppen*, (Teubner, Leipzig 1888).
8. H. De Raedt, and A. Lagendijk, *Phys. Rep.* **127** (1985) 233.
9. M. Suzuki, *Quantum Monte Carlo Methods*, edited by M. Suzuki, (Solid State Sciences 74, Springer, Berlin, 1986).

10. H. De Raedt and W. von der Linden, *Monte Carlo Methods in Condensed Matter Physics*, edited by K. Binder, (Springer, Berlin, 1992).
11. The norm of a matrix X is defined by $\|X\| = M^{-1/2}(\mathbf{Tr}\ X^\dagger X)^{1/2}$.
12. M. Suzuki, *J. Math. Phys.* **601** (1985) 26.
13. H. De Raedt, and B. De Raedt, *Phys. Rev.* **A28** (1983) 3575.
14. M. Suzuki, *J. Math. Phys.* **32** (1991) 400.
15. K. Michielsen and H. De Raedt, "Electron Focussing", Multimedia Presentation.
16. H. De Raedt and K. Michielsen, "Andreev Reflection", Multimedia Presentation.
17. K. Michielsen and H. De Raedt, "Quantum Mechanics", Multimedia Presentation.
18. M. Abramowitz and I. Stegun, *Handbook of Mathematical Functions*, (Dover, New York 1964).
19. The case $n = 9$ is even simpler than the other eight cases but for the sake of brevity, a discussion of this detail is omitted.
20. H. De Raedt, and K. Michielsen , *Computers in Physics* **8** (1994) 600.
21. P. de Vries, H. De Raedt, and A. Lagendijk, *Comp. Phys. Commun.* **75** (1993) 298.
22. N. García, J.J. Sáenz, and H. De Raedt, *J. Phys.: Condens. Matter* **1** (1989) 9931.
23. H. De Raedt, and K. Michielsen, *Nanoscources and Manipulation of Atoms Under High Fields and Temperatures: Applications*, edited by Vu Thien Binh, N. García and K. Dransfeld, (NATO-ASI Series, Kluwer, 1993).
24. H. De Raedt, K. Michielsen, and T.M. Klapwijk, *Phys. Rev.* **B50** (1994) 631.
25. H. De Raedt, and K. Michielsen, Annalen der Physik (in press).
26. P. de Vries, and H. De Raedt, *Phys. Rev.* **B47** (1993) 7929.
27. M.P. Silverman, *Am. J. Phys.* **61** (1993) 514.
28. M.P. Silverman, *And Yet It Moves: Strange Systems and Subtle Questions in Physics* , (Cambridge, New York 1993).
29. M.P. Silverman, private communication.
30. B_0 is the magnetic field for which the Aharonov-Bohm shift of the interference pattern is equal to π.